Journal of Statistical Physics, Vol. 73, Nos. 3/4, 1993

The van Hemmen Spin Glass Revisited

T. Celik,[1,2] U. H. E. Hansmann,[1,3] and M. Katoot[4]

Received June 25, 1993

We simulated the van Hemmen spin glass model by multicanonical algorithm. The exact results for this mean-field model are reproduced. Physical quantities such as energy density, specific heat, susceptibility and order parameters are evaluated at all temperatures. We also studied an alternate model with short range interactions, which displays the many-valley picture in 2D for random variables having values ± 1.

KEY WORDS: Monte Carlo; multicanonical ensemble; spin glasses; van Hemmen model.

1. INTRODUCTION

In the last few years, the multicanonical ensemble[1,2] has been used extensively for numerical simulations in various computational physics problems. It was originally developed for systems with first-order phase transitions to avoid supercritical slowing down.[3–5] Improvements up to 60 orders of magnitude could be achieved and the method was tested on some analytically solvable models.[6] Other targets for the method are systems with conflicting constraints. For low temperatures these systems split into many thermodynamic states, separated by high tunneling barriers. Multicanonical simulations overcome these barriers by connecting back to the high-temperature states, where on the other hand low-temperature canoni-

[1] Supercomputer Computations Research Institute (SCRI), Florida State University, Tallahassee, Florida 32306, U.S.A.
[2] On leave of the absence from Department of Physics Engineering, Hacettepe University, Ankara, Turkey.
[3] Department of Physics, Florida State University, Tallahassee, Florida 32306, U.S.A.
[4] Department of Physical Sciences, Embry-Riddle Aeronautical University (ERAU), Daytona Beach, Florida 32114, U.S.A.

0022-4715/93/1100-0775$07.00/0

cal simulations tend to get trapped in one of those states. Therefore with the new method the relative weight of the branches can be explored and supercritical slowing avoided. Although for these kinds of systems the method is not as well established as for first-order phase transitions, first promising studies exist for spin glasses,[7–9] the random Ising model,[10] and proteins.[11] It was claimed that the multicanonical algorithm outperforms simulated annealing[12] with respect to ground-state investigations, while the relationship to the canonical equilibrium ensemble remains exactly controlled.[8] This is potentially an important development, as similar computational problems (the so-called NP-complete problems) play an important role for a number of systems in biology, chemistry, physics, engineering, economics, and more. It is therefore of importance to test the performance of the multicanonical algorithm against exact results of these kinds of systems.

One aim of this paper is to perform such a test by simulating the van Hemmen spin glass,[13] which is one of the few analytically solvable models for this class of systems. Unlike the more frequently used Sherrington–Kirkpatrick (SK) model,[14] the exact solution can be obtained without replicas. Its main features are consisten with that of a spin-glass model, except for the metastable ground-state structure. To avoid this disadvantage one may consider a finite-range van Hemmen model as suggested by Binder and Young.[15] Such a model, which would be no longer analytically solvable, may lead the way to nontrivial ground-states. Checking this assumption constitutes the other main objective of the present paper.

The paper is organized in the following way. We first review the van Hemmen model. Then we present our results for the infinite-range model. After showing that the method is able to reproduce the exact solutions, we concentrate on the model with local interactions. At the end we give some conclusions and an outlook on further work.

2. THE VAN HEMMEN SPIN GLASS

A spin glass is a disordered magnetic system with a well-defined freezing temperature T_f such that for $T < T_f$ the magnetic moments are frozen in random orientations without a conventional long-range order.[15] An interesting approach to describe such behavior is the van Hemmen model.[13] It is defined by the Hamiltonian

$$H = -\frac{J_0}{N}\sum_{i,j} S(i)\,S(j) - \sum_{i,j} J_{ij} S(i)\,S(j) - h\sum_{i} S(i) \tag{1}$$

describing N Ising spins interacting with an external magnetic field h and with each other in pairs (i, j). A direct ferromagnetic coupling is incorporated via J_0. The J_{ij} contain the randomness,

$$J_{ij} = \frac{J}{N}[\xi_i \eta_j + \xi_j \eta_i] \tag{2}$$

where the ξ_i and η_j are independent and equally distributed random variables with mean zero and variance one. This distribution of J_{ij}'s is shown[16] to model rather well the Ruderman–Kittel–Kasuya–Yosida (RKKY) interaction[17] in a real metallic spin glass: symmetric and highly peaked at $J_{ij} = 0$. The J_{ij} contain $2N$ independent random variables and describe therefore a random-site problem like the Mattis model,[18] not a random-bond problem like the SK model.[14] But unlike in the Mattis model, where $J_{ij} = J\xi_i \xi_j$, the frustration cannot be transformed away by $\hat{S}(i) = \xi_i S(i)$.

The model has three order parameters,

$$m_N = N^{-1} \sum_{i=1}^{N} S(i), \qquad q_{1N} = N^{-1} \sum_{i=1}^{N} \xi_i S(i), \qquad q_{2N} = N^{-1} \sum_{i=1}^{N} \eta_i S(i) \tag{3}$$

Without a ferromagnetic interaction, i.e., for $J_0 = 0$, the magnetization vanishes, $m_N = 0$, and the order parameters q_{1N} and q_{2N} are combined to give a more relevant order parameter q:

$$q = N^{-1} \langle \tfrac{1}{2}(q_{1N} + q_{2N}) \rangle \tag{4}$$

from which the thermodynamic quantities can be obtained. Using Eq. (3), we can rewrite the Hamiltonian in Eq. (1) as

$$-\beta H = N[\tfrac{1}{2} K_0 M_N^2 + K q_{1N} q_{2N} + B m_N] \tag{5}$$

with $K_0 = \beta J_0$, $K = \beta J$, and $B = \beta h$. In the limit $N \to \infty$ one finds the magnetization and the order parameter satisfy the set of equations

$$m = \langle \tanh\{K_0 m + H + Kq(\xi + \eta)\} \rangle \tag{6}$$

$$q = \langle \tanh\{K_0 m + H + Kq(\xi + \eta)\}(\xi + \eta)/2 \rangle \tag{7}$$

where the solutions (m, q) are obtained by minimizing the free energy functional in a mean-field ansatz. Analytical expressions for the other quantities follow from the above equations.

The main features of this mean-field model are that of a spin-glass model with randomness and frustration, but since the system actually picks

out a Mattis state,[18] it lacks the great multiplicity of metastable states which is considered integral to a true spin glass. But one should keep in mind that even the Edwards–Anderson Ising spin glass does not always have this desired multiplicity. For instance, in $D=2$ the model with Gaussian distribution of the J_{ij}s has only two ground states.[19] The van Hemmen model nonetheless still describes a spin glass and deserves further investigation. Being analytically solvable makes it an attractice candidate for the study of systems with randomness and frustration.

3. RESULTS FOR THE INFINITE-RANGE MODEL

We performed multicanonical simulations of the van Hemmen model on clusters of RISC workstations at SCRI and ERAU. Independent Gaussian distributions for ξ_i and η_i with mean value zero and variance one were created. Simulations with $N=64$, 216, 512, and 1000 spins were easily carried out. On the largest systems we performed one million iterations (which requires a few hours of CPU time on an IBM RISC/6000-320h) to obtain the multicanonical parameters for a flat probability distribution. The smaller systems need significantly less iterations and CPU time. Thermodynamic averages were evaluated over two million iterations, following 2×10^5 iterations of initial runs, although with a disordered starting configuration the multicanonical ensemble is immediately in equilibrium. With these extended statistics we could go well beyond earlier work on this model.[20]

We first considered the pure spin-glass case and set the ferromagnetic coupling $J_0=0$. First tentative runs showed a strong dependence of the measured quantities on the lattice volume and the distribution of the random variables even for large lattices, which was neglected in the older work.[20] In order to take into account these finite-size effects, we simulated

Table I. Ground-State Energy e^0, Order Parameter q^0, and Tunneling Time τ_N^e as a Function of the Lattice Volume for the Infinite-Range Model

N	e^0	q^0	τ_N^e
64	−0.3600(89)	0.6031(78)	708(37)
216	−0.3291(47)	0.5727(46)	3422(271)
512	−0.3253(48)	0.5689(55)	8979(1470)
1000	−0.3193(38)	0.5643(47)	23488(1720)
∞	−0.3181(33)	0.5615(37)	—
Exact	−0.3183...	0.5642...	—

ten realizations with different distributions of random variables for each of the $N=64$, 216, and 512 lattices and five realizations for $N=1000$. To evaluate the performance of our algorithm, we defined the ergodicity time τ_N^e as the average number of sweeps needed to move the energy from $E_{\max}$ to $E_{\min}$ and back. A sweep is defined by updating each spin on the lattice once (in the average). The data, displayed in Table I, are consistent with a straight-line fit ($Q=0.76$), which gives the finite-size behavior $\tau_N^e \sim N^{1.27(3)}$ sweeps. In updates this corresponds to a slowing down $\sim N^{2.27(3)}$. This value is close to the optimal behavior $\sim N^2$ and significantly lower than the values observed for the Edwards–Anderson spin glass.[7-9]

This is a first indication of the lack of a many-valley structure such as the one observed in the multicanonical simulation of the Edwards–Anderson model.[8] This point becomes obvious in the distribution of the order parameter q: there are only two ground states. As an example we display in Fig. 1 this distribution for a realization of $N=1000$ spins. $T_f/J=1$ is the bifurcation point, below which the nonzero ordering sets in and smoothly evolves to its maximum value q^0. Both arms of the order parameter distribution of Fig. 1 become more narrow and δ function-like as the temperature decreases. This is what is expected as the multiplicity of the low-lying excited states decreases toward the unique ground state of the model studied here. The existence of these low-lying excited states is also supported by the linear behavior of the specific heat at low temperatures, which we present in Fig. 2 for $N=1000$. Note the strong dependence on the

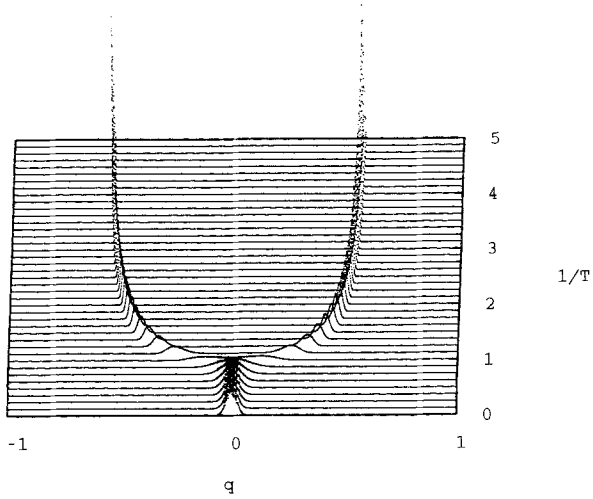

Fig. 1. Spin-glass order-parameter distribution for $N=1000$.

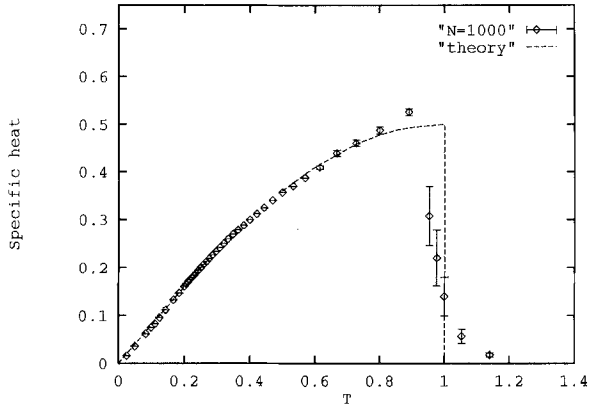

Fig. 2. Specific heat versus temperature for $N = 1000$. The theoretical solution is shown by the dashed line.

distribution of the random variables (hence bigger error bars) around T_f where the model encounters a discontinuity in the specific heat.

We estimate the infinite-volume ground state energy and the ground state value value q^0 of the order parameter from a finite-size scaling (FSS) fit of the form $f_N^0 = f_\infty^0 + c/N$. In Table I we display our results for the different latice sizes. The error bars are with respect to different realizations. Our ground-state energy $e^0 = -0.3181 \pm 0.0033$ is in good agreement with the theoretical value for the infinite lattice $-1/\pi$ at $T = 0$. The same is true for our order parameter value $q^0 = 0.5615 \pm 0.0037$ at $T = 0$, which agrees well with the theoretical value $1/\sqrt{\pi}$.[20]

After having the above-mentioned features of the van Hemmen model assessed by our simulations, we turned to a qualitative investigation of the case with external magnetic field h. We carried out simulations for $0 < h < 1$ with steps of $\Delta h = 0.1$. Figure 3 shows a three-dimensional display of the

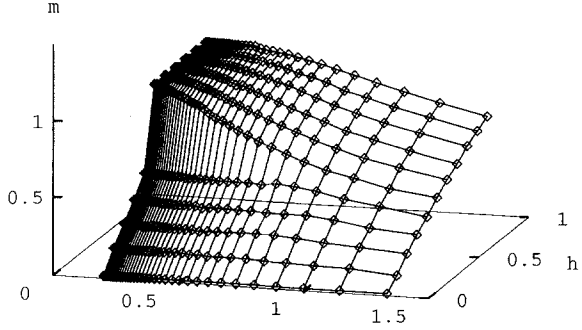

Fig. 3. 3D surface of magnetization versus temperature and magnetic field, obtained from the simulation on an $N = 512$ lattice.

magnetization with respect to temperature and the external field. For $T < T_f = J$, the freezing temperature, a clear jump to a state of higher magnetization is seen for $0.4 < h < 0.5$, indicating a field-induced transition as expected by the analytical results. For $h < 0.4$ we observed the same behavior of the nonzero ordering at temperatures below T_f as displayed in Fig. 1, but found $q = 0$ at all temperatures for $0.5 < h$.

Next we included the ferromagnetic coupling in the model, but with zero external field. The spin glass-to-ferromagnet transition is supposed to take place in the region $J_0 \sim J$. We observed that the magnetization has a jump and the order parameter vanishes for J_0 approaching J. While at $J_0/J = 0.6$ the distribution of the order parameter was the same as depicted in Fig. 1, for $J_0/J = 0.9$ it assumed the value $q = 0.34$ at about $T/J \sim 2$ and stayed constant all the way down to $T = 0$: the system simply keeps staying in the metastable spin-glass phase, and does not jump spontaneously to the ferromagnetic phase. Such a behavior was found elsewhere.[21] Another important quantity is the zero-field susceptibility $\chi_0(T)$. It is shown in Fig. 4 as a function of the temperature for several values of the ferromagnetic coupling J_0. Here the error bars are within the size of the points. One can easily distinguish between two regions. For $T < T_f$ the susceptibility develops a plateau, a feature also shared by the Sherrington–Kirkpatrick model. At $T = T_f$ we find indications for a "cusp" in the susceptibility consistent with a second-order phase transition. The value of the susceptibility at $T = T_f$ agrees well with the analytic solution $\chi_0(T_f) = 1/(J - J_0)$. For $T_f < T$, the susceptibility shows a pure Curie–Weiss behavior $\chi_0(T) = 1/(T - T_f)$. Entering the region of the metastable spin-

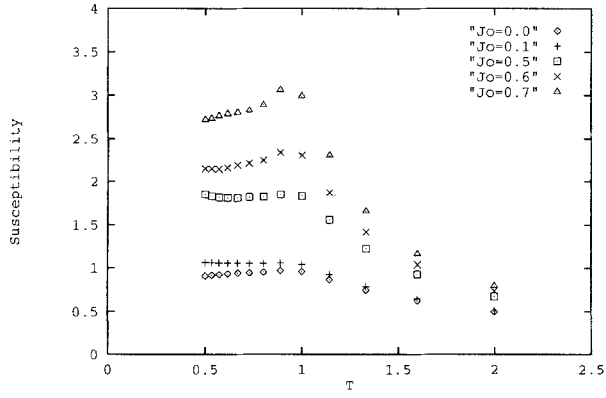

Fig. 4. Susceptibility versus temperature for several values of the ferromagnetic coupling on an $N = 512$ lattice.

glass phase mentioned above, around $J_0/J = 0.6$, the plateau starts getting distorted and only with difficulty can the cusp be recognized.

The multicanonical simulation of the van Hemmen model has produced quite well the results as they are known in the exactly solvable mode. The phases are clearly observed, and main features such as a linear rising specific heat, and the plateau in zero-field susceptibility are easily obtained. We could reproduce with high accuracy the exact values of various quantities for arbitrary temperatures. In our simulations it is straightforward to probe the ground states for systems like the present one which includes randomness and frustration.

4. THE SHORT-RANGE MODEL

What is lacking in the original van Hemmen model is the multiplicity of metastable states, whose absence mainly stems from the long-range character of the interaction. Binder and Young[15] suggested, as a possible way of avoiding this problem, to confine the interaction between pairs (i, j) in the van Hemmen hamiltonian (1) to a finite range. In this section we study the variations of this attempt.

We start our analysis with the nearest-neighbor interaction and continue by stepwise enlarging the interaction range. Both the 2D and the 3D cases are considered. We study mainly the case where the random variables ξ's and η's of Eq. (2) take discrete values ± 1, but also where they are chosen from a Gaussian distribution. From the definition of the J_{ik} in Eq. (2) it follows that the first case, for $D = 2$ with nearest-neighbor interaction, can be interpreted as the site-frustration version of the Edwards–Anderson spin glass, where randomly half of the interactions are suppressed and set equal to zero. Therefore we expect the short-range version of the van Hemmen model to have in this case similar complexity to the Edwards–Anderson model.[22]

If the ξ's and η's are restricted to the values ± 1, the J_{ij} of Eq. (2) can be rewritten as

$$J_{ij} = \frac{J}{N} \xi_i \eta_j (1 + \xi_i \eta_i \xi_j \eta_j) \tag{8}$$

Then the N lattice points can be divided into two disjoint subjects according to the sign of $\xi_i \eta_i$. For $J_0 = 0$, the "blue spins" ($\xi_i \eta_i = +1$) and the "red spins" ($\xi_i \eta_i = -1$) remain as uncoupled sets, since the interaction of Eq. (8) is nonzero only between the spins of the same color. In the mean-field model the Mattis transformation $S(i) \to \xi_i S(i)$ transforms blue ones into ferromagnetic interacting spins and red ones into antiferromagnetic

interacting spins. At sufficiently low temperatures, the blue spins will be ordered, whereas the red spins remain disordered due to frustration.[13] In the short-range model, however, a phase transition can occur only when the ferromagnetic interacting blue spins percolate to form an infinite cluster. This happens when the probability of blue spins exceeds the site-percolation threshold. The dimension then plays as large a role as the site-percolation thresholds depend on it.

We first considered, in $D=2$, the Hamiltonian (1) with sums taken over only the nearest-neighboring pairs (i, j) and $J_0 = h = 0$. The random variables ξ_i and η_i are set with equal probability to ± 1. In this case, the site-percolation threshold is $p_c = 0.59$ and neither the blue spins nor the red spins can form an infinite percolating network. We simulated five realizations with different distributions of random variables for each of the square lattices with $N = 144$, 256, 576 and $N = 1024$ spins. Table II shows our results.

Figure 5 displays the distributions of the order parameter q for one of our realizations with $N = 144$ spins. For temperatures below the bifurcation point the many-valley structure of the ground states, as for the Edwards–Anderson model, reappears. This is what we expected by the above argument and it is the new feature which is missing in the infinite-range version of the model. The model in this form does not form a Mattis state and displays a multiple degenerate ground-state structure. Similar pictures were seen for all of the realizations on the lattices we have studied.

To see the performance of our algorithm for short-range interactions we evaluated the ergodicity times and their finite-size behavior, which are also shown in Table II. A straight-line fit ($Q = 0.51$) to the data gives a slowing down, in updates, of $\sim N^{2.87(22)}$. It is almost a factor N slower than the ergodicity times of the infinite-range model and is related to the fact that the number of local minima increases with the volume, therefore

Table II. Ground-State Energy e^0, Entropy s^0, and Tunneling Time τ_N^e as a Function of the Lattice Volume for the 2D Short Range Model with ξ and $\eta = \pm 1$

N	e^0	q^0	τ_N^e
144	−0.4833(52)	0.0994(26)	11993(2070)
256	−0.4922(18)	0.0977(45)	25565(6702)
576	−0.4929(35)	0.0958(33)	186421(80684)
1024	−0.4932(32)	0.0951(35)	483333(258736)
∞	−0.4956(31)	0.0945(30)	—

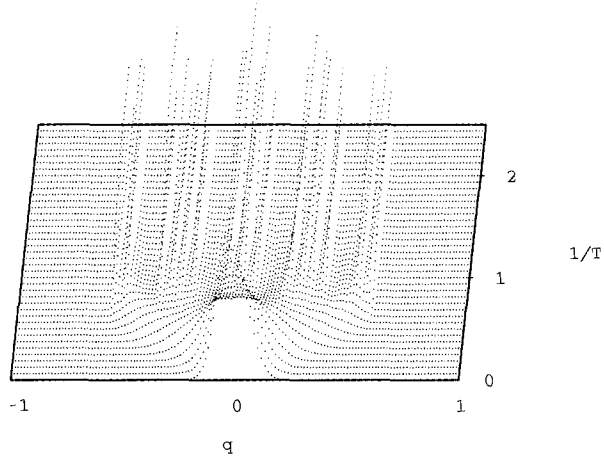

Fig. 5. Short-range van Hemmen model spin-glass order-parameter distribution for $N = 144$.

slowing down the ergodicity time by an extra factor N. On the other hand, our tunneling time is much better than what was achieved in earlier work on multicanonical simulation of the Edwards–Anderson Ising spin glass,[7] the short-range version of the SK model. This reflects also our general observation that simulations of the van Hemmen model are much easier to carry out than the ones of the Edward–Anderson spin glass.

The similarity between the two models can be seen in the specific heat, too. In Fig. 6 we show that the specific heat vs. temperature for $N = 1024$ together with the specific heat for the Edwards–Anderson model.[8] The

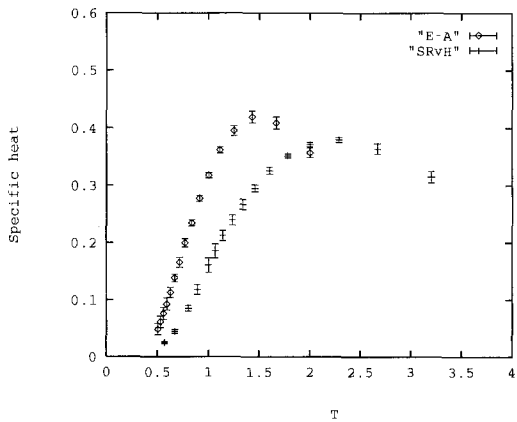

Fig. 6. Specific heat versus temperature for short-range van Hemmen model (SRvH) for $N = 1024$ and for Edwards–Anderson model (E-A) for $N = 2304$.

error bars are with respect to different realizations. The short-range version of the van Hemmen model considered here displays a similar structure to the Edwards–Anderson model and is different from that of the mean-field model as displayed in Fig. 2.

Figures 7a and 7b show the fits for the ground-state energy and entropy per spin. For the ground-state energy we find $e^0 = -0.4956 \pm 0.0031$ compared to $e^0 = -0.5$ for the corresponding infinite-range model with discrete values ± 1 of the random variables. Our estimate for the ground-state entropy is $s_0 = 0.0945(30)$. The approach to scaling seems to take place

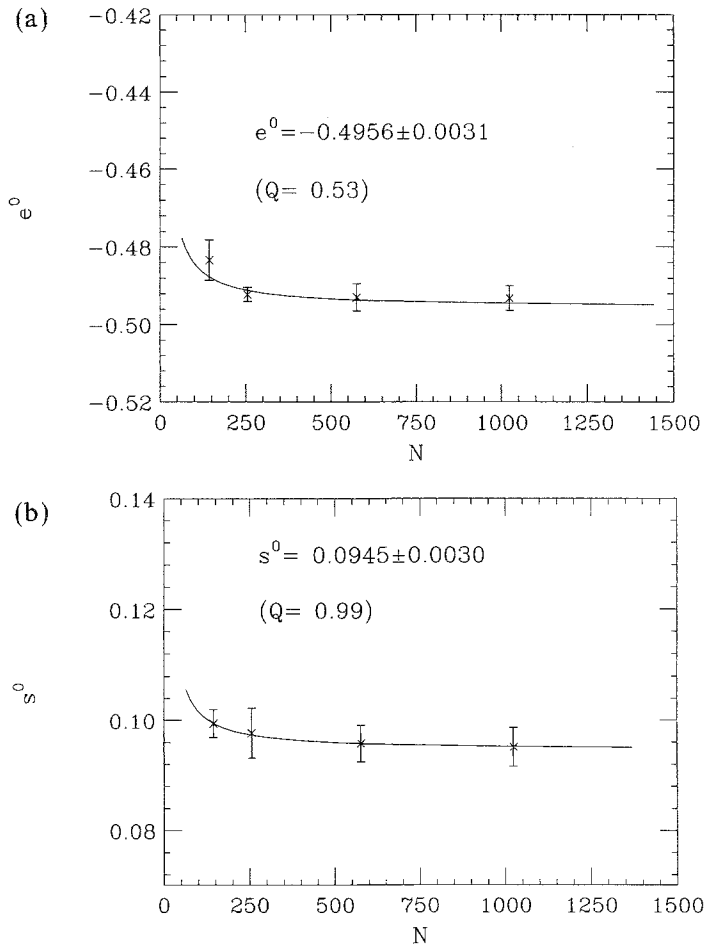

Fig. 7. Estimate of the infinite-volume ground-state energy and entropy for the short-range van Hemmen model with discrete random variables.

already for moderate-size lattices, especially for the ground-state entropy. This is again an indication of multiple degenerate ground-state structure. Our value of the ground-state entropy $s_0 = 0.0951(35)$ for an $N = 1024$ lattice implies 10.6×10^{42} approximate number of distinct ground states.

The important question is then, of course, how does this picture persist. First, staying in 2D, we replaced the ± 1 distributions of the random variables by Gaussian distributions. In this case there were no multiple degenerate ground states and we were back to the two-state feature of the original model. Here, the J_{ij} never vanish and spin clusters are connected by partially frustrated bonds so that the system always forms an infinite percolating network. Again this short-range van Hemmen model behaves in qualitatively similar way to the Edwards–Anderson model. In $D = 2$, the Edwards–Anderson model similarly has a unique ground state for the continuous distribution of random bond variables.[19]

The great importance of the site percolation for our problem can be seen when one keeps the ± 1 distributrion of the random variables, but includes next-to-nearest neighbors in the interaction. Here the site-percolation threshold is $p_c \sim 0.14$.[22] Similarly in 3D with only nearest-neighbor interaction and with ξ's and η's having values ± 1 one has $p_c = 0.312$. Both cases therefore allow infinite clusters of grouped spins. We simulated both cases and found again that the multiplicity of ground states disappear.

We found that the suggestion of ref. 15 did not prove to work as well as expected. Only on a square lattice with nearest-neighbor coupling and with the discrete values ± 1 for the random variables did we obtain multiple degenerate ground states. In this particular case, the frustration does not percolate. Higher dimensions or switching to continuous random variables makes the frustration percolate, and hence a mean-field behavior sets in. Unlike the Edwards–Anderson model, it is not the dimension in which the lattice is embedded, but the site-percolation probability that is the important factor. Hence, the details of the lattice structure are of crucial importance. This restricts the use of the short-range version of the van Hemmen model considered here.

5. CONCLUSION

We tested the performance of the multicanonical algorithm for systems with conflicting constraints by simulating the van Hemmen spin-glass model. We reproduced with high accuracy the values of various quantities as they are known in the exactly solvable mean-field model. This proves that the algorithm is a reliable tool for this class of systems, too, and should encourage its use for other investigations of systems which have

to cope with these kinds of problems. Based on the similarity of the van Hemmen model to neural networks, we intend to use the method here in future work.

To enhance the original model with a richer ground-state structure we also studied, following Binder and Young,[15] variants of the van Hemmen model by replacing the infinite-range interaction. We found in 2D, with discrete random variables and nearest-neighbor interaction, a much richer structure than the original model, but this does not persist in higher dimensions, nor for continuous random variables. Since its behavior depends on the details of the lattice and the interaction, the short-range version of the van Hemmen model does not appear to have a universal character to model spin glasses. This limits the value of such attempts. On the other hand, one may exploit this lattice dependence to construct a spin-glass model with desired structures, but this is beyond the scope of this paper.

ACKNOWLEDGMENTS

This research project was partially funded by the Department of Energy under contract DE-FC05-85ER2500, by MK Industries, Inc., and by the NATO Science Program. T.C. was supported by TUBITAK of Turkey and U.H.E.H. by the Deutsche Forschungsgemeinschaft under contract H180411-1. The authors would like to thank SCRI for its kind hospitality.

REFERENCES

1. B. Berg and T. Neuhaus, *Phys. Lett. B* **267**:249 (1991).
2. G. M. Torrie and J. P. Valleau, *J. Comput. Phys.* **23**:187 (1977).
3. B. Berg and T. Neuhaus, *Phys. Rev. Lett.* **68**:9 (1992).
4. B. Berg, U. Hansmann, and T. Neuhaus, *Z. Phys. B* **90**:229 (1993).
5. W. Janke, B. Berg, and M. Katoot, *Nucl. Phys. B* **382**:649 (1992).
6. B. Berg, U. Hansmann, and T. Neuhaus, *Phs. Rev. B* **47**:497 (1993).
7. B. Berg and T. Celik, *Phys. Rev. Lett.* **69**:2292 (1992).
8. B. Berg and T. Celik, *Int. J. Mod. Phys. C* **3**:125 (1992).
9. B. Berg, T. Celik, and U. Hansmann, *Europhys. Lett.* **22**:63 (1993).
10. E. Marinari and G. Parisi, *Europhys. Lett.* **19**:451 (1992).
11. U. Hansmann and Y. Okamoto, FSU-SCRI-93-12; *J. Comp. Chem.*, submitted.
12. S. Kirkpatrick, C. P. Gelatt, and M. P. Vecchi, *Science* **220**:671 (1983).
13. J. L. van Hemmen, *Phys. Rev. Lett.* **49**:409 (1982); A. C. D. van Enter and J. L. van Hemmen, *Phys. Rev. A* **29**:355 (1984); J. L. Van Hemmen, A. C. D. van Enter, and J. Canisius, *Z. Phys. B* **50**:311 (1983).
14. D. Sherrington and S. Kirkpatrick, *Phys. Rev. Lett.* **35**:1792 (1975); *Phys. Rev. B* **12**:4384 (1978).

15. K. Binder and A. P. Young, *Rev. Mod. Phys.* **58**:801 (1986).
16. K. Binder and K. Schroder, *Phys. Rev. B* **14**:2142 (1976).
17. M. A. Ruderman and C. Kittel, *Phys. Rev.* **96**:99 (1954); T. Kasuya, *Prog. Theor. Phys.* **16**:45 (1956); K. Yosida, *Phys. Rev.* **106**:893 (1957).
18. D. C. Mattis, *Phys. Lett.* **56**:421 (1976).
19. R. N. Bhatt and A. P. Young, *Phys. Rev. B* **37**:5606 (1988).
20. I. Moregenstern and J. L. van Hemmen, *Phys. Rev. B* **32**:6058 (1985).
21. R. B. Griffiths, C.-Y. Weng, and J. S. Langer, *Phys. Rev.* **149**:301 (1966).
22. Ph. de Smedt, J. O. Indekeu, and L. Zhang, *Physica A* **140**: 450 (1987).